



Available online at [www.sciencedirect.com](http://www.sciencedirect.com)

**ScienceDirect**

Publishing Services by Elsevier

International Journal of Naval Architecture and Ocean Engineering 10 (2018) 153–169

<http://www.journals.elsevier.com/international-journal-of-naval-architecture-and-ocean-engineering/>



# PAUT-based defect detection method for submarine pressure hulls

Min-jae Jung <sup>a</sup>, Byeong-cheol Park <sup>b</sup>, Jeong-hoon Bae <sup>b</sup>, Sung-chul Shin <sup>b,\*</sup>

<sup>a</sup> Department of Naval Vessel Service, Korean Register, Pusan, South Korea

<sup>b</sup> Department of Naval Architecture and Ocean Engineering, Pusan National University, Busan, South Korea

Received 8 December 2016; revised 4 April 2017; accepted 8 June 2017

Available online 15 July 2017

## Abstract

A submarine has a pressure hull that can withstand high hydraulic pressure and therefore, requires the use of highly advanced shipbuilding technology. When producing a pressure hull, periodic inspection, repair, and maintenance are conducted to maintain its soundness. Of the maintenance methods, Non-Destructive Testing (NDT) is the most effective, because it does not damage the target but sustains its original form and function while inspecting internal and external defects. The NDT process to detect defects in the welded parts of the submarine is applied through Magnetic particle Testing (MT) to detect surface defects and Ultrasonic Testing (UT) and Radiography Testing (RT) to detect internal defects. In comparison with RT, UT encounters difficulties in distinguishing the types of defects, can yield different results depending on the skills of the inspector, and stores no inspection record. At the same time, the use of RT gives rise to issues related to worker safety due to radiation exposure. RT is also difficult to apply from the perspectives of the manufacturing of the submarine and economic feasibility. Therefore, in this study, the Phased Array Ultrasonic Testing (PAUT) method was applied to propose an inspection method that can address the above disadvantages by designing a probe to enhance the precision of detection of hull defects and the reliability of calculations of defect size.

Copyright © 2017 Society of Naval Architects of Korea. Production and hosting by Elsevier B.V. This is an open access article under the CC BY-NC-ND license (<http://creativecommons.org/licenses/by-nc-nd/4.0/>).

**Keywords:** Submarine pressure hull; Non-destructive testing; Phased array ultrasonic testing

## 1. Introduction

Since the submarine is an underwater, weapons-capable watercraft renowned for its stealthy operation, its hull must be produced such that it can withstand high external water pressure. A pressure hull that can withstand millions of tons of water pressure requires the use of highly advanced shipbuilding technology. It must also be free of defects.

In the US and Australia, countries with submarine design and construction experience, there are numerous cases where welding defects occur in the pressure hull during shipbuilding. Errors in detecting these defects in submarines can jeopardize the lives of the crew and the stability of the ship, and can lead

to unnecessary and costly repairs as well as reduced production capability. Therefore, a rigorous maintenance plan to produce pressure hulls is needed. For producing a submarine hull, each enterprise is required to establish appropriate maintenance programs to conduct periodic inspections and repairs in order to maintain its soundness. Of the maintenance methods, Non-Destructive Testing (NDT) facilitates the detection of internal and external defects in the hull without destroying or damaging the target, and maintains its original form and function. NDT is the most effective maintenance method that can provide appropriate measures in advance.

In Australia, all cracks in pressure hulls that fatally affect their strength are detected by developing methods of ultrasonic testing (Yule and Woolner, 2008). NDT should be reliable and reproducible. NDT is required to convert qualitative results into quantitative results.

In this study, following an analysis of the disadvantages of NDT methods, Phased Array Ultrasonic Testing (PAUT) is

\* Corresponding author.

E-mail address: [scshin@pusan.ac.kr](mailto:scshin@pusan.ac.kr) (S.-c. Shin).

Peer review under responsibility of Society of Naval Architects of Korea.

applied to supplement their disadvantages. The result is the proposal of a probe design to enhance the precision of defect detection and the calculation of defect size. Hence, this study can contribute to the establishment of standards for accurate soundness evaluation and their on-site application to submarine pressure hulls.

## 2. Types of NDT on submarine pressure hull

The pressure hull of a submarine consists of a pressure hull frame, a mid-assembly block and a large-assembly block welded together. The quality of the welding can be guaranteed by the application of NDT. This is the first step in quality assurance and is a core process for providing fundamental data for the soundness evaluation of the welded parts of the pressure hull. Therefore, NDT requires reliability of detection above all. Its application to submarine manufacture involves the observance of NDT procedure, the use of a qualified inspector, and the fulfillment of certain requirements regarding the condition of inspection equipment. These factors vary with the inspection criteria of the shipbuilding company.

When a welding defect occurs in the pressure hull, it can critically damage to the strength of the structure. Defects can be divided into surface and internal defects. MT (magnetic particle testing) is conducted to detect defects on and under the surface of the welded parts of the pressure hull, whereas Radiography Testing (RT) and Ultrasonic Testing (UT) are used to detect internal defects.

### 2.1. MT

MT is a method to detect surface defects by generating a magnetic field and observing the magnetic particles resulting from the distortion in the magnetic flux to detect defects. When magnetizing a ferromagnetic target, a magnetic leakage field is generated. When magnetizing a ferromagnetic target, a magnetic leakage field is generated on the indication and then indications are formed in parts generated by the magnetic leakage field. By using these indications, tissue changes or defects in the target material can be detected (HRDKOREA, 2015).

The principle underlying MT is to detect the generation of magnetic leakage flux, or changes in permeability triggered by the tissue's status and the existence of discontinuity, when the target is placed in a magnetic field and is magnetized. Fig. 1 shows the principle of magnetic particle inspection (ASNT,

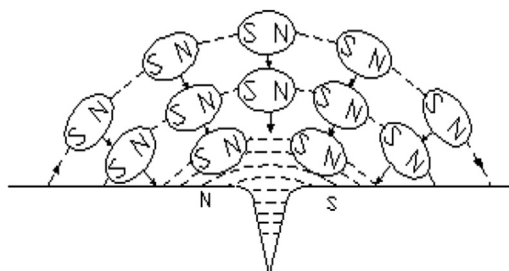


Fig. 1. Principle of magnetic particle inspection.

1989). When magnetic particles collect at a flux leakage site, they produce a defect that is visible to the unaided eye under proper lighting conditions. One of the most important properties of magnetic materials is permeability. Permeability can be thought of as the ease with which materials can be magnetized. More specifically, permeability is the ratio between the flux density and the magnetic field strength (ASNT, 1989). Fig. 2 shows the magnetic permeability (Sehwa, 2001).

### 2.2. UT

The basic principle underlying UT is that high-frequency ultrasonic waves can penetrate a material. Using the feature whereby ultrasonic waves are reflected from a boundary layer composed of different substances, the ultrasonic wave is emitted into the target and reflected, if a defect exists. UT uses a probe device to decipher the reflected wave on a Cathode Ray Tube (CRT) screen to detect the existence, location, and size of the defects. Imaging is carried out using the A-Scan. When an ultrasonic wave generated by the probe is fed into the target, because of the difference in the acoustic impedance of the materials, some reflected and penetrated ultrasonic waves are refracted, in accordance with Snell's Law, as shown in Fig. 3. The location of the defect is measured by the time taken to receive the transmitted ultrasonic wave, whereas the size of the defect is measured by the echo height of the ultrasonic wave or by the range where the defect echo occurs. Since ultrasonic waves are also reflected by the defect, the defect echo, which is not observed within the target, is observed between the transmission echo and the basal echo.

### 2.3. RT

RT is a method to determine the existence of defects by transmitting X-rays and Gamma-rays through the target and using images formed on a film. The strength of the radiation weakens due to interaction with materials constituting the target as it penetrates the target. At the time, the intensity of radiation changes due to the internal structure of the target. The change in the intensity of radiation is reflected on the film to identify defects. Imaging is carried out using the C-Scan (2-D view of ultrasonic data displayed as a top or plan view of the test specimen).

When porosity of size  $\Delta r$  exists in a target due to the thickness of T, the X-ray radiated from its focus is dispersed

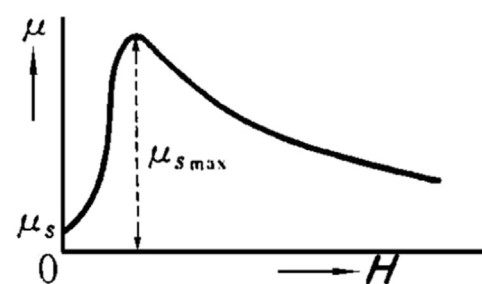


Fig. 2. Magnetic permeability.

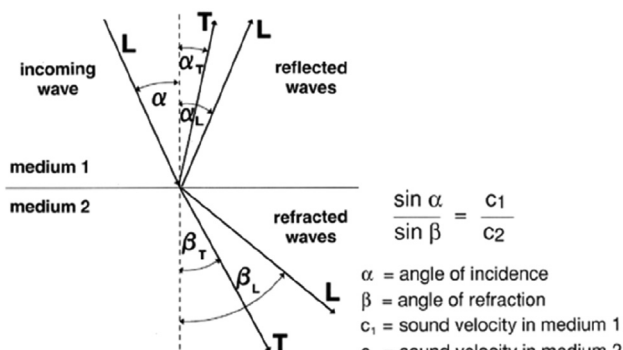


Fig. 3. Snell's law.

widely onto the target. The intensity of the direct transmission penetrating defect  $I'$  can be represented by Eq. (1):

$$I' = I_o \cdot e^{-\mu(T-\Delta T)} \quad (1)$$

$\mu$ : linear absorption coefficient ( $\text{cm}^{-1}$ )

$\Delta T$ : thickness of porosity

$I_o$ : intensity of incident x-ray

$I'$ : intensity of the direct transmission penetrating defect

### 3. NDT standard for submarine pressure hull

The pressure hull of a submarine contains a fully penetrated butt weld. According to the NDT standards for each country, surface defects in the same welded part should be detected using MT. Moreover, the use of NDT to detect internal defects is commonly recommended in conjunction with that of UT and RT. However, the characteristics of the detected parts (material thickness, parts with concentrated stress, etc.) are different in each country. In this section, the NDT standards for a submarine pressure hull are compared by country.

#### 3.1. NDT standards for pressure hull by country

As mentioned above, MT is commonly applied for NDT to detect surface defects in the welded parts in each country. However, the methods to detect internal defects differ from country to country.

In Germany, for internal defect detection of the welded parts of the pressure hull, RT, and UT are separately applied according to the thickness of the material. DNV-GL (2015) uses RT for the circumferential joint and longitudinal joint of the pressure hull and applies UT to the other welded parts. This is the result of considerations whereby in parts such as the head and the stern, where the constituting materials are thick, the sensitivity of the film is low when the same amount of radiation is transmitted, and comparatively reduces detection capability.

In Australia, all welded parts of the pressure hull are subjected to UT (Yule and Woolner, 2008). However, the application of UT and RT overlap in some welded parts (approximately 10% of all parts). This indicates that some parts such as those where stress is concentrated and others, where automatic welding is not used and the likelihood of welding defects is relatively high, are subjected to overlapping detections.

In France (BV, 2009) and the U.S. (NAVSEA, 1997), UT or RT can be applied selectively. In France, instead of RT, the partial application of additional UT is possible. However, when all parts are subjected to UT, an approval from a publicly certified institute is required. The NDT standards for welded parts, as regulated by each country, are shown in Table 1.

#### 3.2. Analysis of NDT standard for pressure hull

The comparison among NDT standards of countries showed that the differences can be set as articles ‘①: Overlapping RT’ and UT and ‘②: Single RT or single UT’. With the application of the Nuclear Safety Act, South Korean domestic safety regulations have been considerably reinforced. Radiographic test using an X-ray device or radioisotope (Ir 192) must now be conducted within only the “dedicated workplace appropriate for radiological protection countermeasures” or the “covering facility or cover for radiation protection” (Jo, 2014). RT is concerned with workers' safety issues arising out of radiation exposure. Since the working time of RT is long, and since it cannot be combined with production work, there are several hurdles in the route to satisfying the standards of the article ①, in terms of the

Table 1  
Criteria of NDT for submarine's pressure hull.

Country	MT	RT	UT
Germany	Surface	Butt weld full penetration	Butt weld full penetration
	100%	(100% Weld thickness $\leq 100 \text{ mm}$ )	(100% Weld thickness $> 100 \text{ mm}$ )
DNV-GL	Surface	Butt weld (longitudinal, circumferential) (RT 100%)	Except for RT point
	100%		
Australia	Surface	10% of the weld on the pressure hull	Butt weld (UT 100%)
	100%		
U.S.	Surface	RT or UT Full penetration welds	
	100%		
France	Surface	Butt weld (RT 100%)	Butt weld, full penetration (UT 100%)
	100%	A partial replacement of radiography by ultrasonics is permitted provided that the required length is tested. Complete replacement of radiography with ultrasonics is subject to the agreement of the society.	

manufacturing process of submarines, economic feasibility, and the risk of radiation exposure.

When approached from the perspective of detection capability, in accordance with the article ②, RT, and UT are different in terms of their principles for detecting defects. Therefore, there might be a difference in their capabilities of defect detection. Moreover, since the prevalent UT depends on the experience and knowledge of a skilled inspector, when analyzing ultrasonic signals in the equipment, the skill of the inspector can greatly influence results, which can also be affected by underlying conditions of the inspection. Moreover, the recording and storage of the inspection are challenging tasks, because of which there are problems in terms of detailed analysis using the same data. Therefore, additional plans for NDT are direly needed in order to enhance the reliability and accuracy of the soundness evaluation of submarine's pressure hull, while complementing the above disadvantages due to inspection standards ① and ②.

#### 4. Application of PAUT

To supplement the disadvantages of UT and RT when applied to the soundness evaluation of a submarine pressure hull, and in order to develop cutting-edge NDT technology to provide quantitative data, PAUT is applied. Moreover, a PAUT probe was designed to improve the detection capability on a submarine's pressure hull.

##### 4.1. Characteristics of PAUT

By applying a time delay to arrange piezoelectric elements in PAUT, the progressive direction of ultrasonic waves can be adequately adjusted by using Huygens's Principle. Each piezoelectric element in the probe is adjusted by computer-controlled excitation. Depending on the external input, pulses can be independently transmitted and received by each piezoelectric element. The probing beam of a single piezoelectric element is spread along a single direction, whereas the

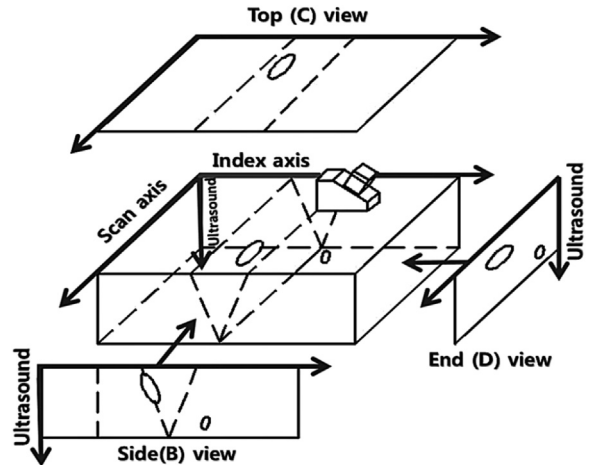


Fig. 5. Scanning views of A-, B-, C-, D-scan.

PAUT probe, comprising multiple probes, is capable of detecting cracks from multiple directions due to the irradiation of the beams at various angles and their concentration. Fig. 4 shows Huygens' principle for a plane wave (a) and for a spherical wave (b) (Cliffsnotes, 1918).

##### 4.2. Scanning views of PAUT

PAUT refers to an electronic processing method wherein each small piezoelectric element receives ultrasonic signals. This allows for the real-time acquisition of images of the inside of a specimen. A PAUT probe consists of multiple small elements, each of which can accept ultrasonic signals via electronic processing. Hence, PAUT can acquire images of the inside of the material in real time. One of the advantages of PAUT is the ability to obtain images of defects without scanning along the index axis.

Ultrasonic views are images defined by different plane views between the ultrasonic path and scanning parameters (scan or index axis). The most important view, similar to 2-D projections of a technical drawing, is presented in Fig. 5. Such

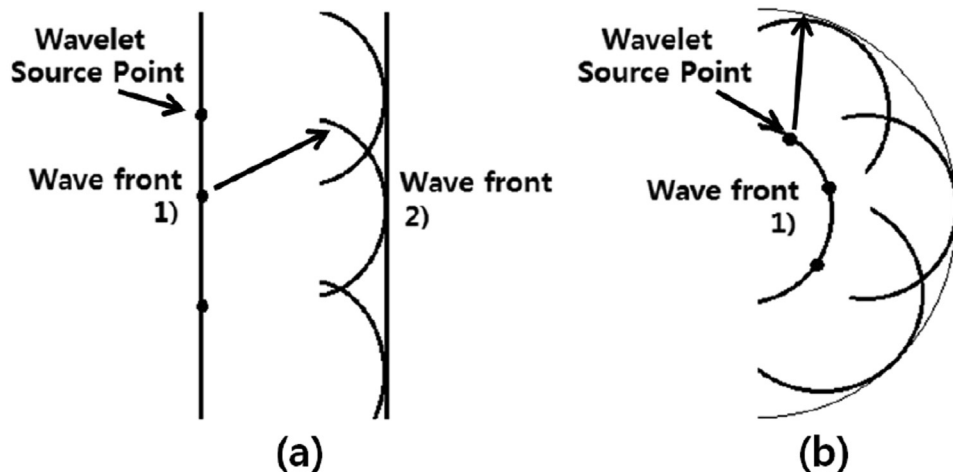


Fig. 4. Huygens' principle for (a) a plane wave and (b) a spherical wave.

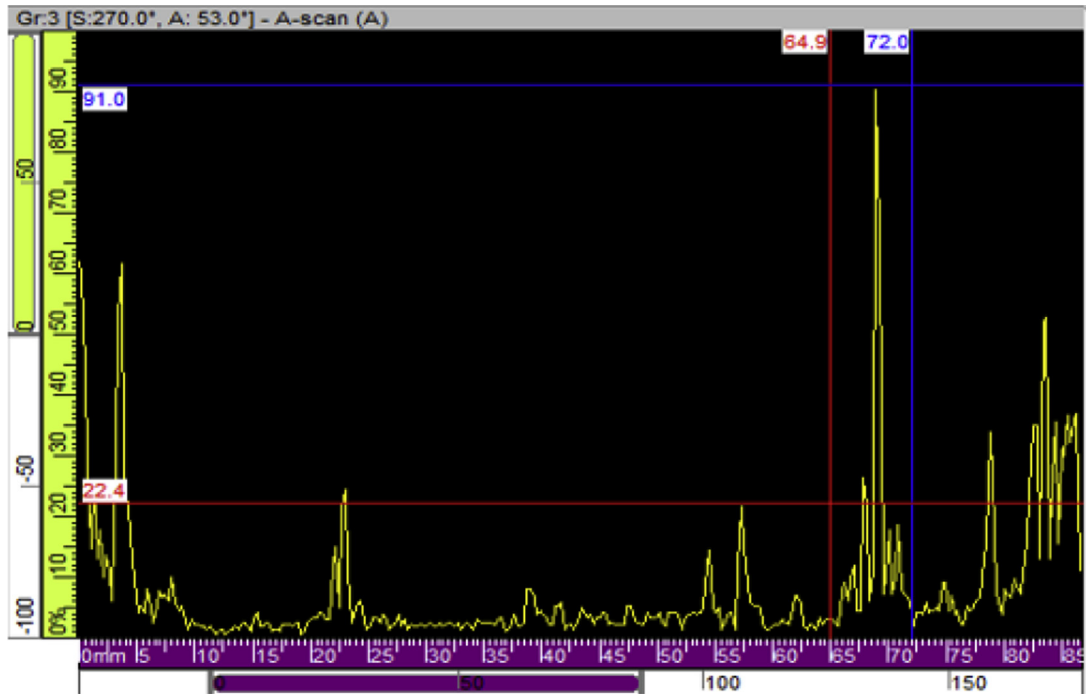


Fig. 6. Example of A-scan representation.

projection views are a plan or cumulated plans obtained via C-scan, B-scan, and D-scan; the projection views are also called top, side, and views (Olympus NDT, 2004). In addition, the A-(raw data), B-, C-, and D-scan analysis can be performed on a single screen, allowing easy identification of the shape and location of defects (see Fig. 6).

#### 4.2.1. A-scan

The A-scan is a wave pattern commonly shown in conventional UT as Fig. 6. The reflective wave is directly

displayed on the screen without being processed upon reception. Also known as a waveform, an A-scan is a graphical representation of the received ultrasonic pulse amplitude versus the time of flight (Ultrasonic path), or a waveform. An A-scan can be displayed as an RF (Radio-frequency) or bipolar-rectified signal (Olympus NDT, 2004).

#### 4.2.2. B-scan

A B-scan shows the entire signal information on a single screen after saving the A-scan signals received in a probe. The

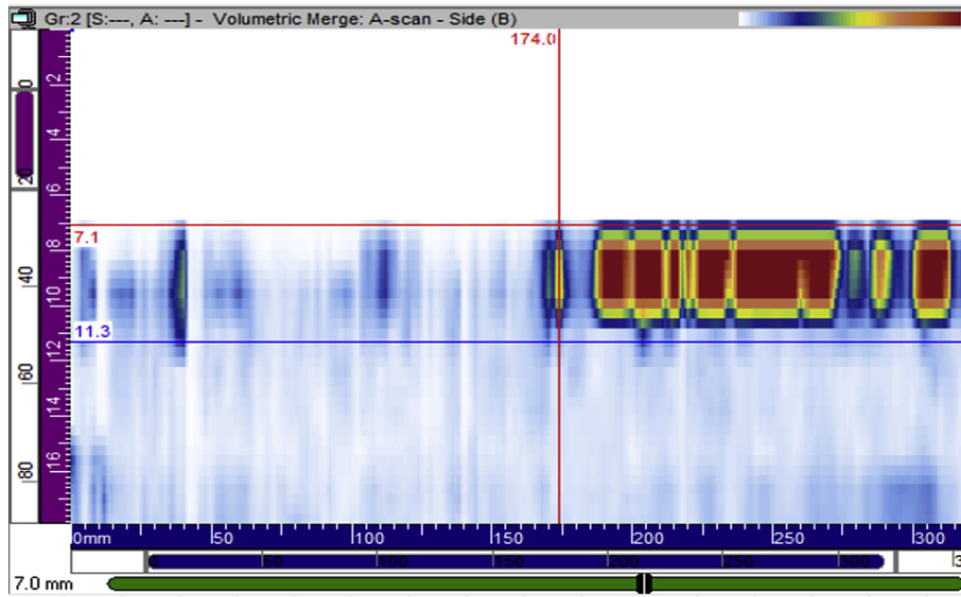


Fig. 7. Example of B-scan representation.

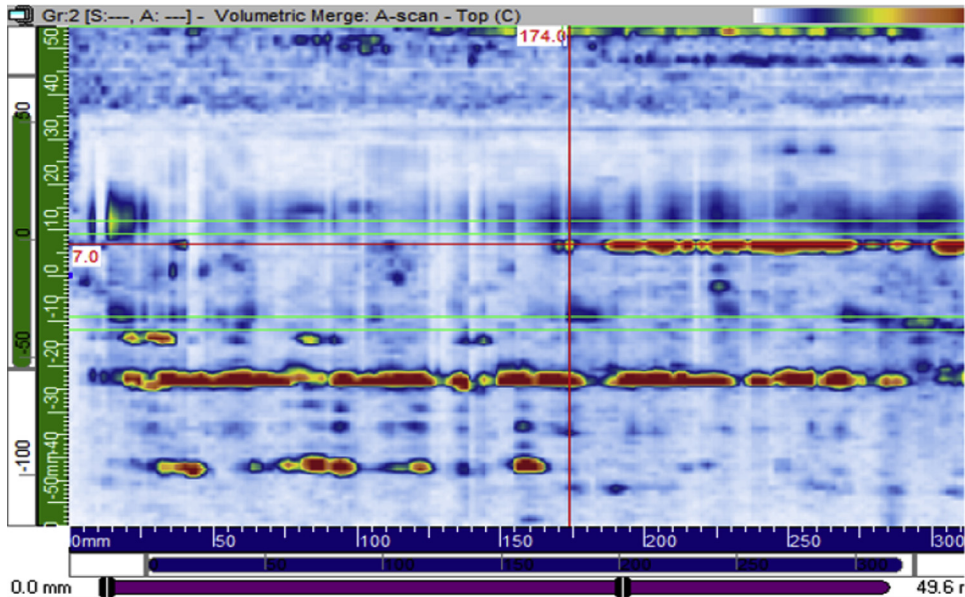


Fig. 8. Example of C-scan representation.

B-scan is a 2-D view of recorded ultrasound data. Usually, the horizontal axis represents the scan position and the vertical axis represents the ultrasound path or time, as shown in Fig. 7. The axes can be reversed, depending on the required display. The position of the displayed data is related to the encoder positions at the moment of acquisition. Essentially, a B-scan is a series of stacked A-scans or waveforms. Each A-scan is represented by an encoder/time-base sampling position. If the ultrasonic path is corrected owing to the refracted angle and delay, the B-scan will represent the volume-corrected side view of the inspected part, with scan length on the horizontal axis and depth on the vertical axis (Olympus NDT, 2004) (see Fig. 8).

#### 4.2.3. C-scan

A C-scan is a 2-D view of ultrasonic data displayed as a top or plan view of the test specimen as shown in Fig. 8. One of the axes is the scan axis and the other is the index axis. With conventional ultrasonic systems, both axes are mechanical, and with linear-phased arrays, one axis is mechanical, while the other is electronic. The position of the displayed data is related to the encoder positions during acquisition. Only the maximum amplitude for each point is projected on this “scan-index” plan view, technically known as a C-scan (Olympus NDT, 2004).

#### 4.2.4. D-scan

A D-scan is similar to a B-scan, but the view is at a right angle to that of the B-scan as shown in Fig. 9. As a two-dimensional graphical presentation of data, one of the axes is defined as the index axis and the other is defined as the ultrasonic path. If the B-scan is a side view, then the D-scan is an end view. The B-scan displays scan axis versus time, whereas the D-scan displays index axis versus time (Olympus NDT, 2004).

### 4.3. Designing PAUT probe device

PAUT can obtain images of ultrasonic waves by adjusting the focus and direction of the wave beam. The PAUT probe comprises multiple piezoelectric elements, and is configured with design variables such as wavelengths, number of piezoelectric elements, and width.

Of the defects in a submarine's pressure hull, porous and crack defects are the most critical defects in terms of stress concentration and strength. To enhance the precision of detecting these defects, which are to be avoided at all cost from the perspective of stress concentration and strength, design variables that consider the removal of the grating lobe, the interference effect of the waves, and focus the ultrasonic wave were selected. The performance of the probe, which reflected the above design variables, was verified through a simulation. The defect detection capability of the verified probe was quantitatively evaluated by an experiment. Fig. 10 shows phased array probe design variables (KSNT, 2013) (Fig. 9).

#### 4.3.1. Improvement in beam focusing and beam steering

The beam-focusing of ultrasonic waves is the concentration of acoustic energy into a small focal spot, and is an important element for increasing the resolution of defects in the pressure hull during PAUT probing. For optimized beam focusing for accurate defect detection in the pressure hull, the number of piezoelectric elements among the design variables was selected, and the local acoustic field was hence confirmed to analyze the defect detection zone. The center frequency was set to 5 MHz and modeling was conducted for 16, 32, and 64 piezoelectric elements, based on the beam tool.

When 16 piezoelectric elements were used, the near field was 30 mm; when 32 piezoelectric elements were used, the near field was 133 mm; when 64 piezoelectric elements were

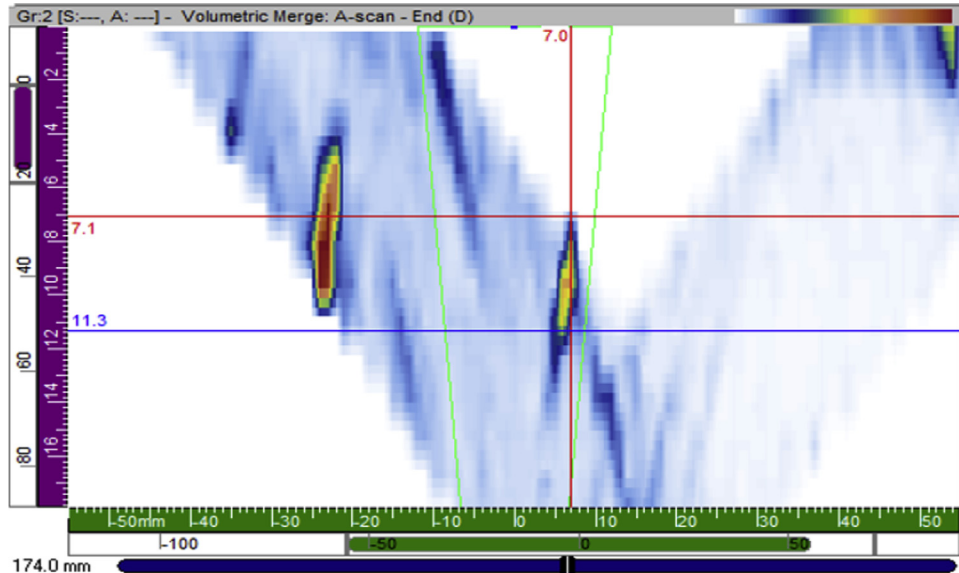


Fig. 9. Example of D-scan representation.

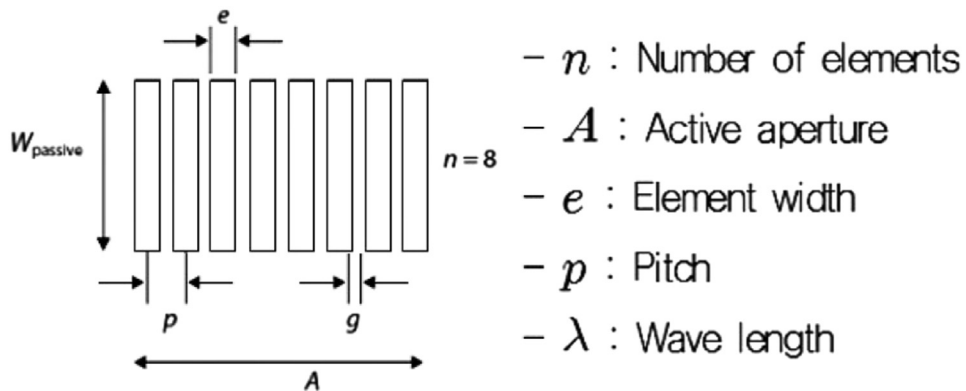


Fig. 10. Phased array probe design variables.

used, the near field was 546 mm. This shows that the near field was widest when 64 piezoelectric elements were used. The results of the modeling are shown in Fig. 11.

The defect detection capability of the PAUT probe was enhanced by removing the grating lobe, which is diffraction interference relevant to the contents of this study. Interference occurs in each piezoelectric element, and its elimination should be considered as early as in the design stage of the probe. Therefore, modeling for different numbers of piezoelectric elements was conducted, and the results are shown in Fig. 12.

As the number of piezoelectric elements increased, favorable defect detection results were derived, based on results from the reduced grating lobe through the diffraction effect (see Fig. 13). Therefore, it was found that the number of piezoelectric elements greatly influenced the range of detection. Fig. 12 shows the grating lobe dependence on the number of elements (Kim, 2007).

#### 4.3.2. Results of PAUT probe design

Considering the best performance in terms of beam focusing and beam steering, the most suitable number of piezoelectric elements was 64 and the most suitable frequency 5 MHz, for piezoelectric elements used to detect defects in the submarine's pressure hull.

The width and pitch of the piezoelectric element were set to 0.5 mm and 0.6 mm, respectively, by minimizing the width of the piezoelectric element, in order to not generate the grating lobe by considering the range of detection. The maximum size of the piezoelectric element according to the maximum refraction angle was verified in accordance with Eqs. (2)–(6).

$$e < 0.67\lambda = e < 0.67 \times 1.18 = e < 0.79\text{mm} \quad (2)$$

$$e < \lambda/2 = 1.18/2 = e < 0.59\text{mm} \quad (3)$$

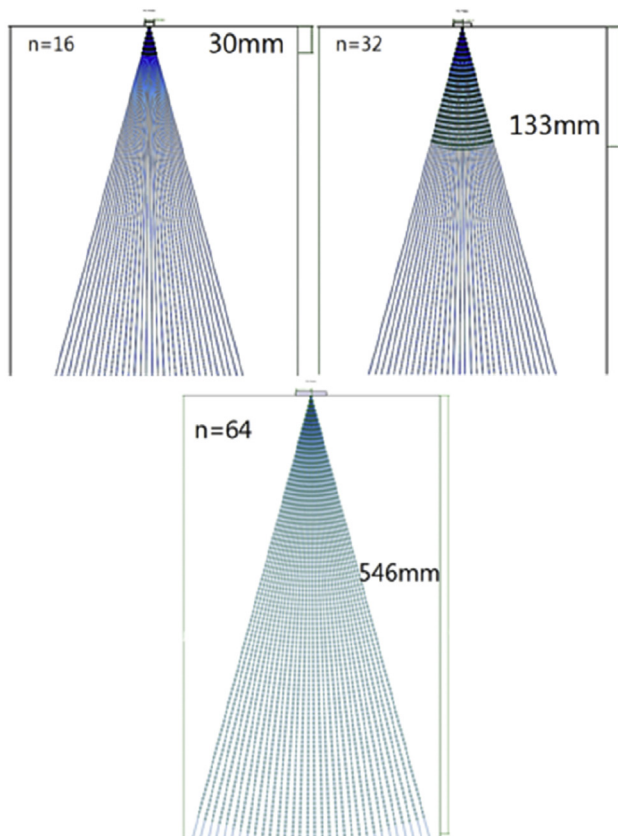


Fig. 11. Result of near field dependence on number of element.

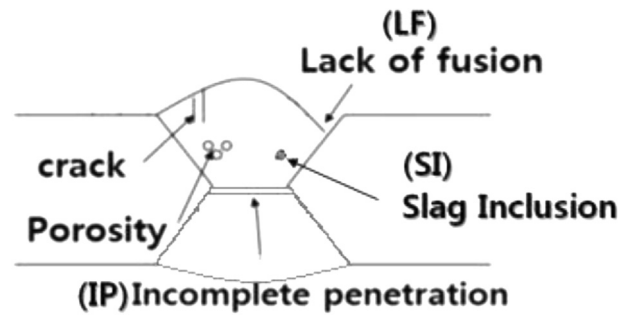


Fig. 13. Welding defects of specimen.

$$e_{\max} = 0.514\lambda/\sin\beta_{R\max} = 0.514 \times 1.18/\sin 70^\circ = 0.64\text{mm} \quad (4)$$

$\sin \beta_{\max}$ : maximum refraction angle [°]

$$\rho > \lambda/2 = 1.18/2 = 0.59\text{mm} \quad (5)$$

$$e + g = 0.5 + 0.1 = 0.6\text{mm} \quad (6)$$

From Eq. (6), as the length of the active aperture increased, better sensitivity and focal constant were obtained. Since the local acoustic field zone was proportional to the length of the active aperture, the maximum active aperture of 38.4 mm was applied as Eq. (7).

$$\text{Max. active aperture} = \rho \times n = 0.6 \times 64 = 38.4\text{mm} \quad (7)$$

$\omega_{\text{passive}}$  is a variable related to the length and depth of the narrow beam. Its validity, in relation to the length of the designed active aperture and appropriateness, was verified in accordance with Eqs. (8) and (9).

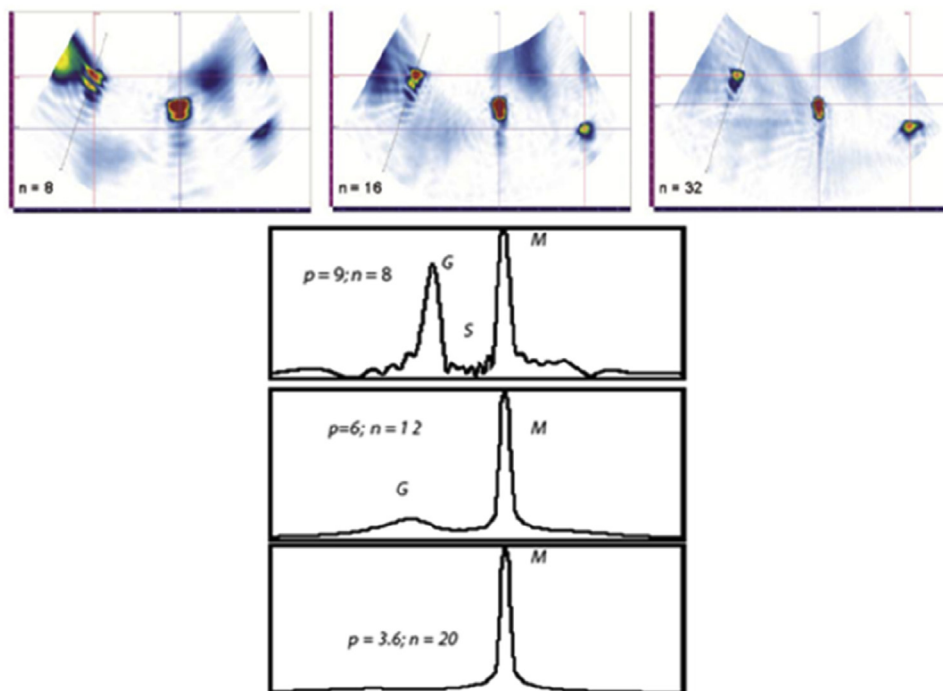


Fig. 12. Grating lobe dependence on number of element.

Table 2  
Parameter design of PAUT probe.

Parameter design	Value
f (Frequency)	5.0 MHz
n (Number of elements)	64
A (Active aperture)	38.4 mm
e (Element width)	0.5 mm
p (Pitch)	0.6 mm
g (Element gap)	0.1 mm
ω (Passive aperture)	10.0 mm

$$A > \omega_{\text{passive}}, \omega_{\text{passive}} > 10p \quad (8)$$

$$38.4\text{mm} > 10\text{mm}, 10\text{mm} > 10 \times 0.6 = 6\text{mm} \quad (9)$$

The parameters of the PAUT probe were derived according to the calculation results, yielded by considering design variables of the probe such as beam focus and steering. The results are shown in Table 2.

## 5. Experiment

### 5.1. Manufacturing the specimen

In order to assess the defect detection capability of the proposed method and conduct a quantitative evaluation, various forms of specimens were manufactured in accordance with the conditions stated in formal welding specifications.

The material thickness was set to 30 T, considering the average thickness of the existing submarine's pressure hull. The material thickness was then set to 40 T, considering the local thickness with strength required by the submarine's pressure hull (see Fig. 13).

Five types of welding defects—porosity, lack of fusion, incomplete penetration, crack, and slag inclusion—were selected to manufacture 17ea defects. The detailed information is shown in Fig. 13.

### 5.2. Equipment

The experiment was conducted using NDT equipment owned by DSME (Co., Ltd.), and the detailed information is as follows:

#### 5.2.1. RT

In RT, the X-ray device TOSHIBA EX-220 GH-3 was used. The density was set to 2.0–4.0, and a strength of 39 Ci was applied.

#### 5.2.2. UT

In UT, an Olympus NDT EPOCH XT MSEB 4-type was used as probe, and its frequency was set to 4 MHz. The angles were 45°, 60°, and 70°.

#### 5.2.3. PAUT

PAUT used the probe conditions stated in Section 4.2, and wedged by an angle ranging from 40 to 70°, using the SA2-N55S and SA2-0L types. To determine a method to accurately

evaluate the length of the defect, additional experiments were conducted for each type of acoustic pressure drop method.

## 6. Results and discussion

17 different types of welding defects in the 30T and 40T specimens were examined by conducting RT, UT, and PAUT to measure the location, length, and depth of each defect (in terms of the X- and Y-axes). Here, the X-axis refers to the horizontal distance between the left end of the material and the beginning point of the defect, and the Y-axis refers to the vertical distance between the center of the weld bead and the defect. Furthermore, the defect length is defined as the difference between the beginning and the end points of the welding defect in the X-axis direction, and the defect depth is defined as the difference between the top and bottom ends of the defect, as shown in Fig. 14.

### 6.1. Results of specimen 40T

Table 4 summarizes detailed data on the location, length, and depth of defects (1)–(5) in the 40T.

Defects (1) and (2) were not detected using RT, but using PAUT (see Fig. 15 and Fig. 16). Their detailed locations and sizes were identified from A-, B-, C-, and D-scans. The results of the scans are summarized in Fig. 17 and Fig. 18.

The A-scan indicates the received amplitude of the UT path, with the highest point of the echo pointing to defects (1) and (2). The B-scan represents the depth and the probe movement axes, from which the X-axis from the side and the defect depth were inferred. For (1), the depth is 4.5 mm and the X-axis is 0.0 mm; for (2), they were 6.5 mm and 6.0 mm, respectively.

In the C-scan, the horizontal axis is the scan axis and the vertical axis is the index axis. This type of scan enables data collection of the X- and Y-axes of the defect from the top view. The results indicate that the X- and Y-axes are 0.0 mm and −3.4 mm for (1), respectively, and 6.0 mm and 4.4 mm for (2), respectively.

The D-scan defines the depth and the electronic scan axis and reveals the defect depth and the Y-axis from the end view. The depth and the Y-axis values are 4.5 mm and −3.4 mm, respectively, for (1), and 6.5 mm and 4.4 mm for (2), respectively.

Defects (6)–(12) were created in the 40T. Details on the location, length, and depth of defects (6)–(12) are summarized in Table 5.

Fig. 19 and Fig. 20 show the results for defects (6)–(12) for the 40T obtained from RT and PAUT, respectively. In Fig. 20, the image located outside the green line, which represents the weld bead, represents the discontinuity in the parent material and is thus irrelevant to the welding defects. Here, the discontinuity refers to an interruption of the typical structure of a material. A discontinuity is not necessarily a defect.

Defects (6), (11), and (12) were detected not using RT, but using PAUT, and their detailed locations and sizes were identified by the A-, B-, C-, and D-scans. The results

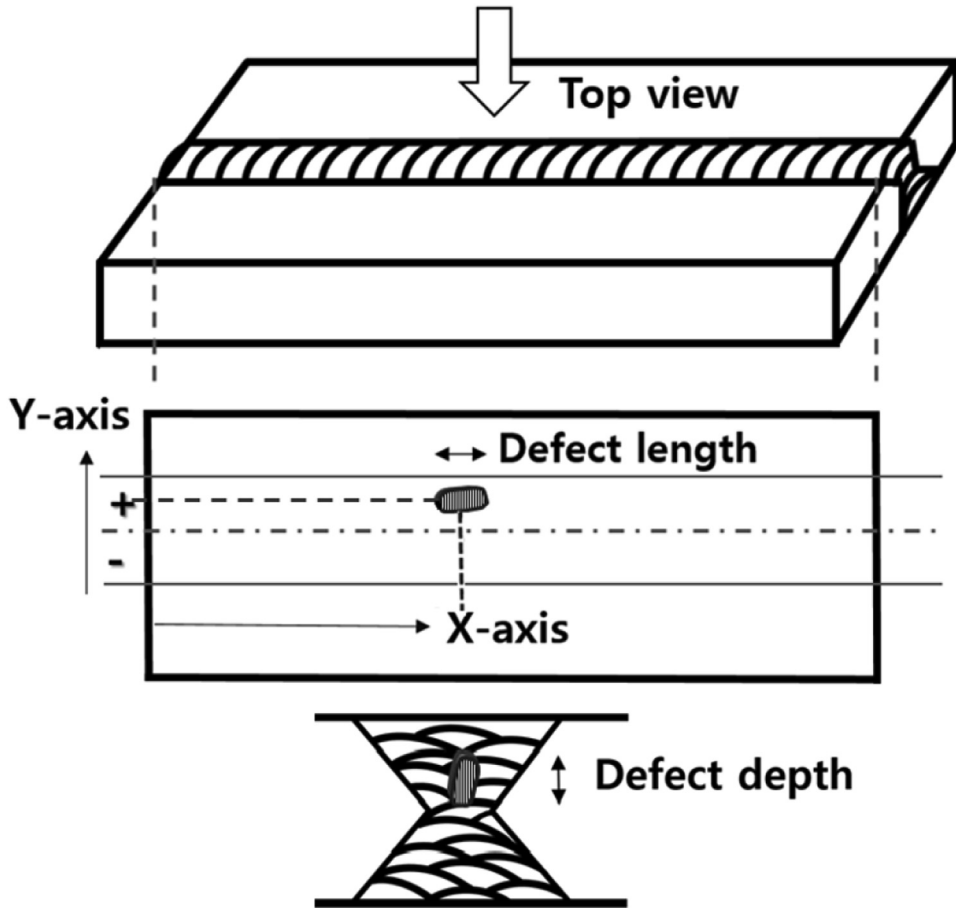


Fig. 14. Length, position, and depth of welding defect.



Fig. 15. Experimental result of defects (3)–(5) obtained using radiographic testing (C-scan).

are presented in Figs. 21–23, respectively Figs. 24 and 25.

The B-scan shows that the depth and X-axis value of the defects are 6.0 mm and 0.0 mm for (6), 3.0 mm and 125.0 mm for (11), and 3.0 mm and 13.0 mm for (12), respectively.

The C-scan shows that the X-axis and Y-axis values of the defects are 0.0 mm and 3.4 mm for (6), 0.0 mm and 3.4 mm for (11), and 142.0 mm and -6.8 mm for (12), respectively.

Finally, the D-scan shows that the depth and Y-axis value of the defects are 6.0 mm and -0.4 mm for (6), 3.0 mm and

Table 4  
Experimental result of defects obtained using RT, UT, and PAUT (40T).

Defect type	NDT	Defect length (mm)	Defect location (mm)		Defect depth (mm)
			X-axis	Y-axis	
(1) IP	RT	undetected			
	PAUT	6.0	0.0	-3.4	4.5
(2) IP	RT	undetected			
	PAUT	9.0	6.0	4.4	6.5
(3) Crack	RT	17.0	65.0	unknown	
	PAUT	24.0	58.0	2.2	6.6
	UT	22.0	57.0	2.5	4.5
(4) Porosity	RT	15.0	118.0	unknown	
	PAUT	11.0	122.0	2.2	7.0
	UT	10.0	122.5	2.5	4.5
(5) LF	RT	155.0	165.0	unknown	
	PAUT	162.0	155.0	-4.0	5.0
	UT	160.0	155.0	-4.5	4.5

Table 3  
Parameters of PAUT probe.

Material	HY-100
Material thickness	30T, 40T
Welding joint/groove	X-groove
Welding process	Flux Cored Arc Weld (FCAW)

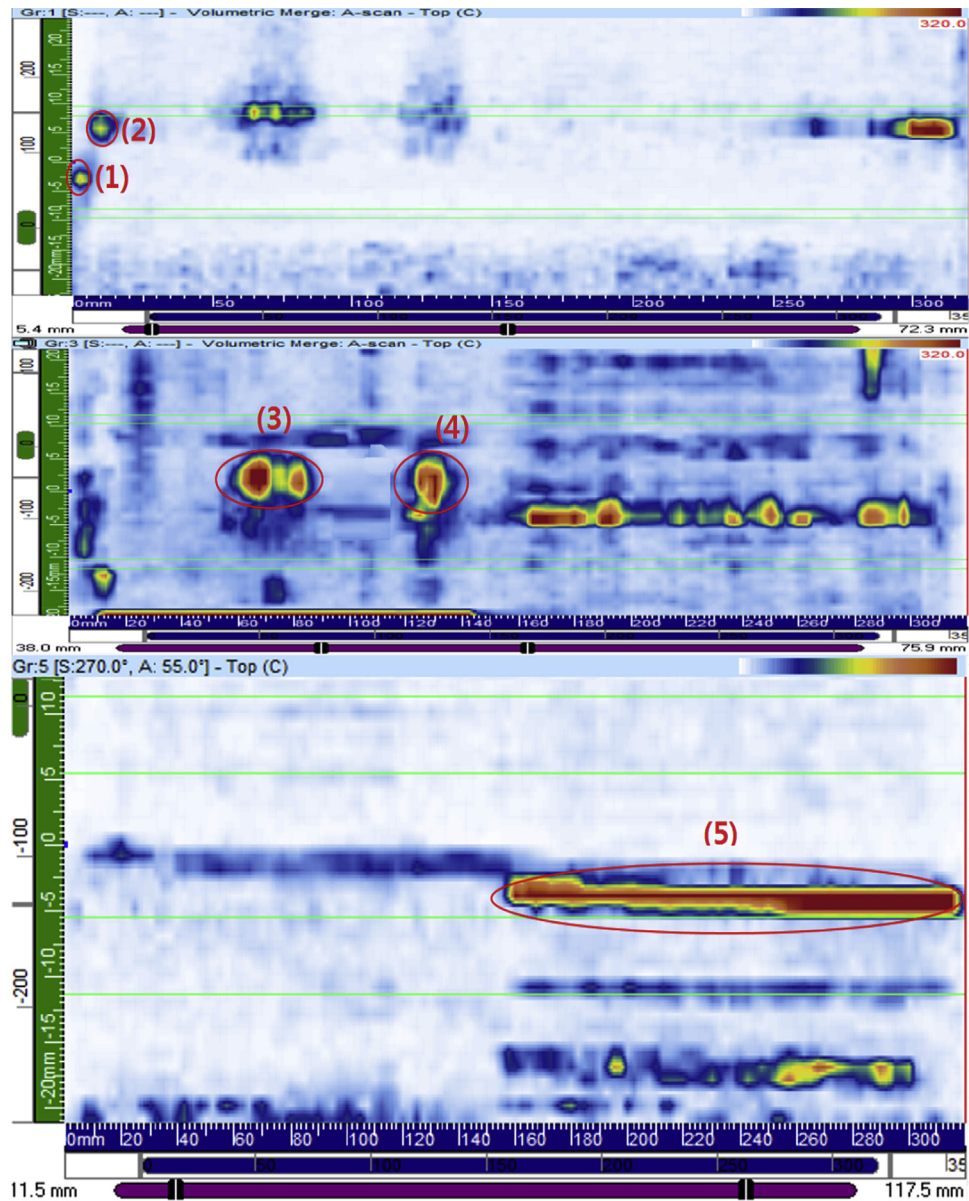


Fig. 16. Experimental result of defects (1)–(5) obtained using phased-array ultrasonic testing (C-scan).

–6.8 mm for (11), and 3.0 mm and –6.8 mm for (12), respectively.

#### 6.2. Results of specimen 30T

Defects (1)–(5) were created in the 30T material. Details on the location, length, and depth of defects (6)–(12) are summarized in Table 6.

#### 6.3. Comparative analysis of experimental result

In RT, conducted on the 40T specimen, no linear defect for (1), (2), (6), (11), and (12) was detected. In PAUT, all 12ea defects were detected. Since the beam of the radioactive ray emitted from the linear source was vertically irradiated onto

the specimen, the central part of the radiated beam was vertical. However, at the end of the beam, the detection of lateral direction became weak because of the scattering of the beam, as in (1), (2), and (6). In cases (11) and (12), in RT, the irradiation angle became large along the direction of the linear defect. Since the gap among the defects was narrow, the difference in the thickness of the penetration decreased, which in turn led to a failure to detect defects. The defect in (7) was 2 mm longer in UT than in RT, whereas the defects in (3), (5), (7), and (10) were 7 mm longer. In terms of porosity, (4) and (9), RT was 2–6 mm longer than PAUT. This was deemed as a problem occurring during the measurement of the round defect caused by the scattering of the ultrasonic wave beam, due to the size of the piezoelectric element in UT. On the contrary, in case (8), despite the volumetric defect, RT was 2 mm longer

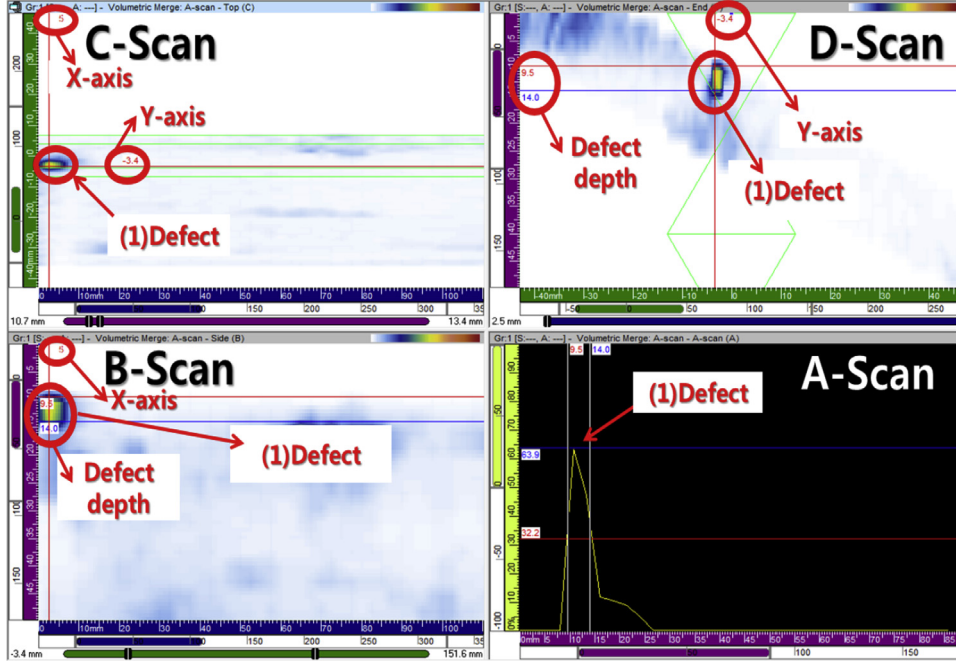


Fig. 17. Experimental result of defect (1) obtained using phased-array ultrasonic testing (A-, B-, C-, D-scan).

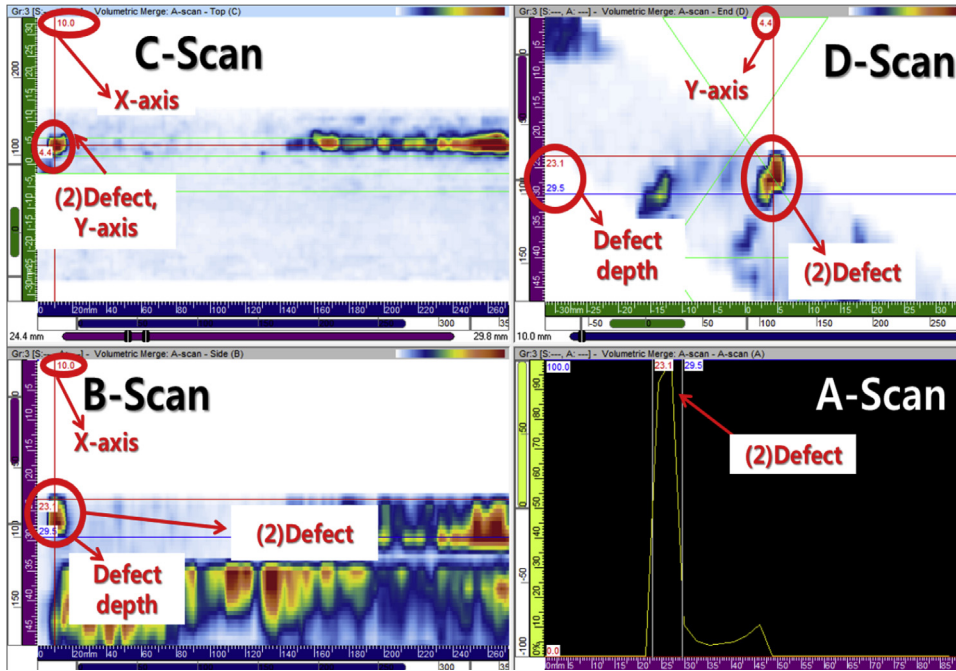


Fig. 18. Experimental result of defect (2) obtained using phased-array ultrasonic testing (A-, B-, C-, D-scan).

than PAUT, showing high accuracy. This was because of excellent beam focusing, derived from the increased number of piezoelectric elements. Tables 7 and 8 are the result of defect length.

Although the existing UT yielded results similar to those for PAUT, cases (8) and (9) were erroneous. Furthermore, in the existing UT, the derivations of location and depth were

available, as in PAUT. However, when the defects were mixed, there were difficulties in deriving accurate values. Therefore, the information was calculated using the ranges of location and depth, or were approximated. On the contrary, PAUT automatically detected accurate location and depth values for each defect, which were deemed the deviations in results triggered by the skill level of the inspector in UT. Moreover,

Table 5

Experimental result of defects (6)–(12) obtained using RT, UT, and PAUT (40T②).

Defect type	NDT	Defect length (mm)	Defect location (mm)		Defect depth (mm)
			X-axis	Y-axis	
(6) Crack	RT	undetected			
	PAUT	1.0	0.0	-0.4	6.0
	UT	undetected			
(7) Crack	RT	3.0	10.0	unknown	
	PAUT	5.0	9.0	5.6	5.0
	UT	4.0	10.0	1.5	4.0
(8) Porosity	RT	22.0	20.0	unknown	
	PAUT	24.0	21.0	-5.8	12.0
	UT	8.0	25.0	-1.0	10.0
(9) Porosity	RT	38.0	68.0	unknown	
	PAUT	32.0	70.0	4.2	13.5
	UT	8.0	80.0	2.5	10.0
(10) SI	RT	19.0	123.0	unknown	
	PAUT	20.0	123.0	5.2	12.0
	UT	15.0	127.5	2.5	9.0
(11) SI	RT	undetected			
	PAUT	15.0	125.0	-6.8	3.0
	UT	10.0	130.0	-1.0	—
(12) SI	RT	undetected			
	PAUT	13.0	147.0	-6.8	3.0
	UT	9.0	155.0	-1.0	—

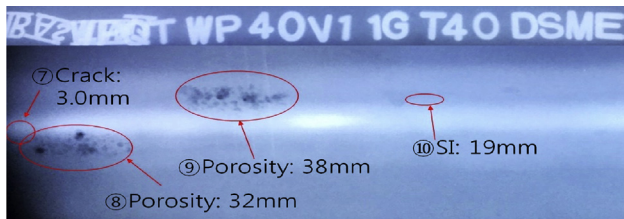


Fig. 19. Experimental result of defects (7)–(10) obtained using radiographic testing (C-scan).

the UT applied the raster scan method to detect defects, thus using more than 3.5 h for inspection, whereas PAUT applied linear scan that took less than half an hour. Therefore, PAUT enhanced detection speed by more than seven times over UT.

In specimen 30T, the linear defects of (2) and (5) were 1 mm longer in PAUT than in RT. The reason for the reduction in length in comparison with the 40T specimen was that detection sensitivity increased with thickness in RT. In case of defect (1), PAUT yielded a length 27 mm greater than RT did. This indicated that PAUT, with better beam focus and steering, detected defects undetected in RT and that the length increased due to the pattern of ultrasonic wave refraction.

The 6ea defects undetected in RT were confirmed in terms of length, location, and depth by various imaging methods in PAUT. The detailed results are as follows:

#### 6.4. Analysis of method for the calculation of defect length using acoustic pressure drop

In order to calculate the length of the defect using ultrasonic waves, the probe was moved from the point yielding the

maximum echo amplitude as acoustic pressure decreased, to calculate the length of the defect. The acoustic pressure drop normally applied 6 dB drop, 12 dB drop, and overall drop. By using signals obtained from the PAUT probe, the length of each defect was additionally calculated for each drop method. By using the results, the method used to assess the defect length of the submarine's pressure hull was analyzed.

In general, the 12 dB drop and the overall drop showed greater lengths than the actual length and results included in the lengths of defects located nearby. The 6 dB drop, which reduced echo by 1/2 (6 dB) at the point yielding the maximum echo amplitude, showed results similar to the actual results, whereas precision was enhanced to the extent of measuring a range of 3 mm. Therefore, the 6 dB drop was verified as the most reliable method for measuring the defect length of the submarine's pressure hull.

#### 6.5. Analysis of results and future improvement

Using PAUT, a probe was applied to yield improved defect detection capability on the submarine's pressure hull. The probe addressed the disadvantages of prevalent NDT. Moreover, the method used to calculate the size of defects was experimentally tested and reliability was verified as below:

- 1) The performance of the PAUT probe for detecting defects in the submarine's pressure hull was analyzed by a simulation. The results showed that the PAUT probe, arranged with 64 piezoelectric elements capable of generating ultrasonic wave at angles of 40°–70°, and set with 0.5 mm as the width of the piezoelectric element and 5.0 MHz as frequency, was the optimal. It was proved that no acoustic intervention occurred at any angle. By applying the probe based on the beam propagation model, defects 1 mm long and 3 mm deep could be detected. The detection capability of porous and crack defects, which are the most critical in the manufacture of submarine pressure hulls, improved as well.
- 2) RT was unable to detect some crack defects, due to its characteristics whereby the beam scatters on the edge of the specimen. Hence, its relative detection capability decreased as the thickness of the specimen increased. On the contrary, in PAUT, the number of piezoelectric elements was increased to 64 in order to increase the range of depth of acoustic pressure. Hence, the detection of cracks as small as 1 mm became possible. This indicated that the number of piezoelectric elements greatly influences the range of detection.
- 3) Although PAUT showed relatively poorer volumetric defect detection capability than RT, as the number of piezoelectric elements increased to 64, the size of some volumetric defects was elongated by 2 mm over RT, thus enhancing the beam focus.
- 4) RT showed poorer detection capability due to the geometry and orientation of the defects, such as cracks, as the thickness of material increased. On the other hand, PAUT applied angles ranging from 40° to 70° to clearly detect

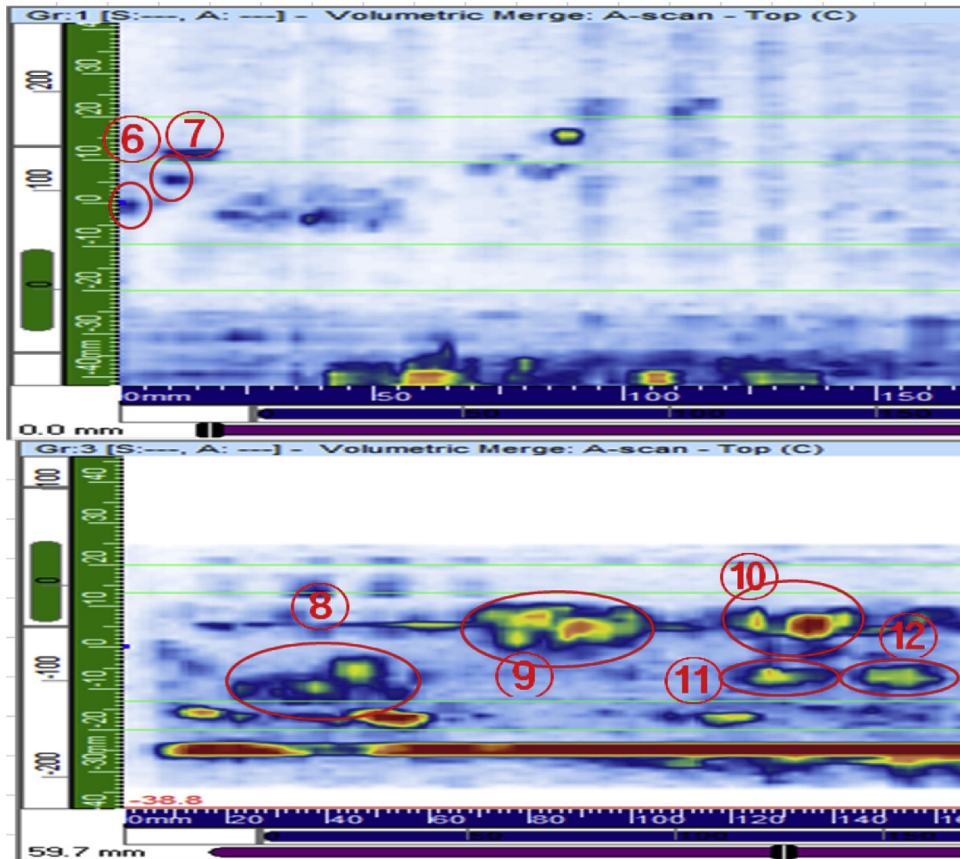


Fig. 20. Experimental result of defects (6)–(12) obtained using phased-array ultrasonic testing (C-scan).

defects in comparison with RT, thus increasing the precision of the detection of cracks.

5) To enhance the measurement accuracy of the defects lengths, the results of acoustic drop method were analyzed.

A 6 dB drop showed results most similar to the actual lengths of the defects. It also showed that the measurement could cover a range of up to 3 mm. Therefore, the reliability of the proposed 6 dB drop was verified.

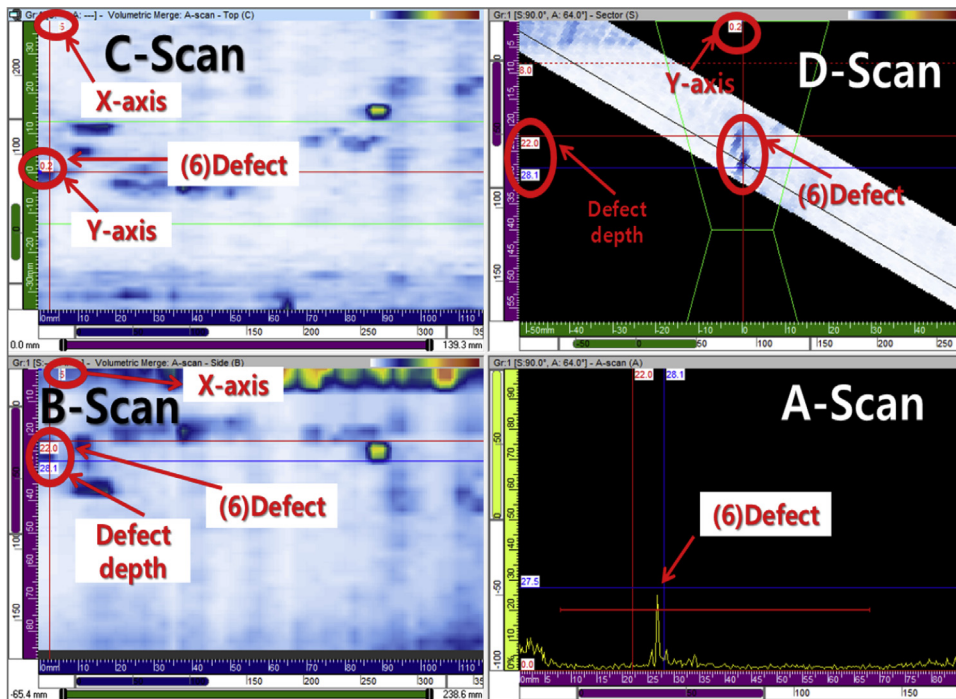


Fig. 21. Experimental result of defect (6) obtained using phased-array ultrasonic testing (A-, B-, C-, D-scan).

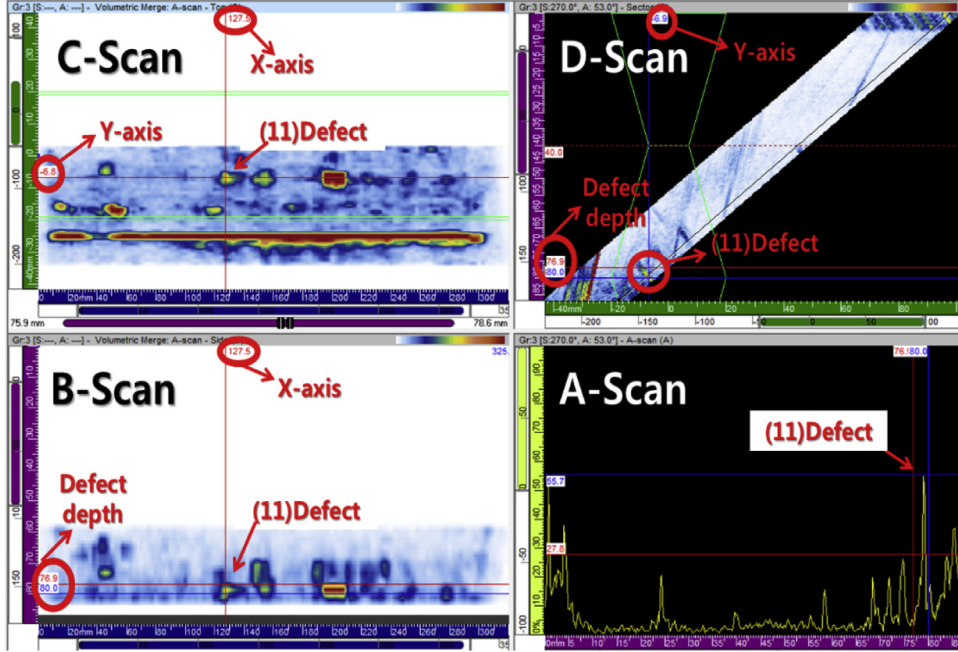


Fig. 22. Experimental result of defect (11) obtained using phased-array ultrasonic testing (A-, B-, C-, D-scan).

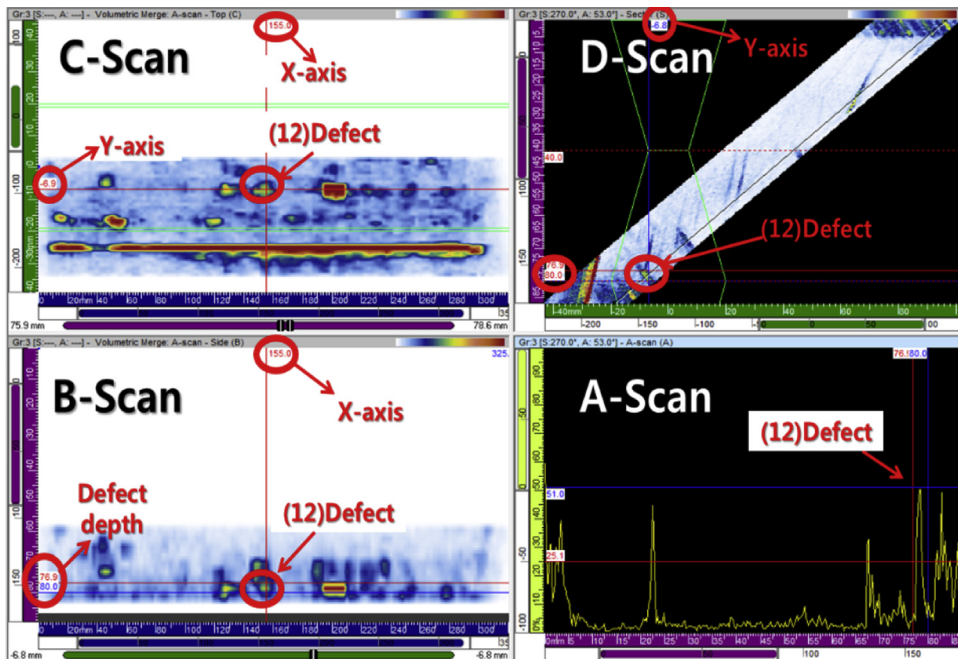


Fig. 23. Experimental result of defect (12) obtained using phased-array ultrasonic testing (A-, B-, C-, D-scan).



Fig. 24. Experimental result of defects (2)–(5) obtained using radiographic testing (C-scan).

- 6) The existing UT showed deviations in mixed defects or defects at low height according to the skill of the inspector. On the other hand, PAUT depended less on the inspector's skill. Moreover, by improving resolution using the probe, rear refraction was applied, even to a defect height of 1 mm in mixed defects, in order to enable imaging using the S-scan.
- 7) The existing UT was unable to record and store the results of a single A-scan at a predetermined incident angle, whereas RT was able to conduct a passive analysis of defect

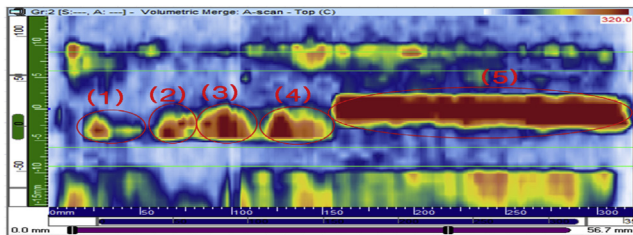


Fig. 25. Experimental result of defects (1)–(5) obtained using phased-array ultrasonic testing (C-scan).

Table 6  
Experimental result of defects using RT, UT, and PAUT (30T).

Defect type	NDT	Defect length (mm)	Defect location (mm)		Defect depth (mm)
			X-axis	Y-axis	
(1) Crack	RT	3.0	26.0	undetected	
	PAUT	30.0	20.0	-3.4	4
	UT	10.0	25.0	-1.0	4–5
(2) Crack	RT	17.0	59.0	undetected	
	PAUT	18.0	58.0	-3.4	4
	UT	6.0	62.5	-1.0	4–5
(3) Crack & Porosity	RT	32.0	81.0	undetected	
	PAUT	34.0	80.0	-3.4	4
	UT	7.0	85.5	-1.0	4–5
(4) IP & Porosity	RT	16.0	119.0	undetected	
	PAUT	36.0	118.0	-3.4	4
	UT	35.0	121.5	-1.0	4–5
(5) IP	RT	161.0	154.0	undetected	
	PAUT	162.0	154.0	0.6	7.1
	UT	162.0	154.0	0.0	5.0

Table 7  
Measuring result of defect length (30T).

Defect type	6 dB (mm)	12 dB (mm)	Fully (mm)
(1) IP	6.0	7.0	11.0
(2) IP	9.0	10.0	15.0
(3) Crack	24.0	28.0	32.0
(4) Porosity	11.0	13.0	17.0
(5) LF	162.0	164.0	168.0
(6) Crack 1	3.0	10.0	15.0
(7) Crack 2	5.0	7.0	13.0
(8) Porosity	24.0	40.0	49.0
(9) Porosity	32.0	37.0	48.0
(10) SI	20.0	45.0	49.0
(11) SI	15.0	Including result of defect (10)	Including result of defect (10)
(12) SI	13.0	Including result of defect (10)	Including result of defect (10)

Table 8  
Measuring result of defect length (40T).

Defect type	6 dB (mm)	12 dB (mm)	Fully (mm)
(1) SI	30	36	41
(2) Crack	18	104	111
(3) Porosity	34	166	170
(4) Porosity	36	—	—
(5) SI	162	—	—

length and the x-axis results using the film of the C-scan. On the other hand, PAUT automated the analysis of data for positive locations and the depth of each defect. By using various imaging methods, A, B, C, and S-scan, the results were recorded. Therefore, the reliability of testing and the precision of defect evaluation were verified.

8) In the existing UT, raster scan was applied, whereas PAUT used electrical linear scan, more than seven times faster. The improvement in detection speed was thus verified. PAUT did not encounter any issues regarding radiation exposure, and thus was proven to be the advanced technology in terms of safety. The reduction in detection time will yield high efficiency in the manufacturing process of submarines.

## 7. Conclusions

RT and UT are NDT methods for detecting the internal defects of a submarine's pressure hull. They are limited in terms of their safety, workability, reliability, and detection time. Therefore, in this study, by applying the PAUT method, the disadvantages of prevalent NDT methods were supplemented, numerous technical enhancements were made to improve quality assurance in the manufacture of submarine pressure hulls by improving the detection capability of porosity and cracks, and the reliability of the calculation of defect size was improved. In particular, to reinforce the beam-focusing of the ultrasonic wave, the number of piezoelectric elements in PAUT was increased to 64 to verify the enhanced precision of defect detection for porosity and cracks.

By applying 40°–70° as the testing angles of the piezoelectric elements to expand the detection range, the defects undetected in RT were detected in PAUT probing. The length of the crack was significant and was observed clearly, indicating the improvement in beam-steering capability.

From the aspect of detecting defects in submarine pressure hulls, a 6 dB drop was used to obtain a range of detection of 3 mm, thus proving precision and reliability.

In future, in order to enhance defect detection capability further, a greater number of piezoelectric elements for the probe will be used, optimization studies on various design variables will be conducted, and additional methods will be developed to calculate clear defect size to further enhance the reliability of soundness evaluation of the welded parts of the submarine's pressure hull. By applying the PAUT method, significant benefits are expected in terms of enhanced quality assurance in submarine hull manufacture.

## Acknowledgement

This work was supported by the National Research Foundation of Korea(NRF) grant funded by the Korea government(MSIP) through GCRC-SOP (No. 2011-0030013).

## References

ASNT, 1989. Nondestructive Testing Handbook (Magnetic Particle Testing). Columbus, USA.

- BV, 2009. Rules for Classification Naval Submarines, Part C Pressure Hull and Structures. Paris, France.
- Cliffsnotes, 1918. Wave Optics. <https://www.cliffsnotes.com/study-guides/physics/light/wave-optics>.
- DNV-GL, 2015. DNV GL Rules for Classification: Naval Vessels (RU-NAVAL). Report No. DNV-GL-RU-NAVAL. Det Norske Veritas, Oslo, Norway.
- HRDKOREA, 2015. Nondestructive Inspection II. Ulsan, Korea.
- Jo, J.B., Jung, K.S., Jang, Y.S., Hur, S.S., 2014. Phased array ultrasonic examination in lieu of radiography to comply with the new nuclear safety law. *Int. J. Steel Struct.* 26 (5), 57–60.
- Kim, Y.S., 2007. A Study on Flaw Evaluation for Turbine Disk Rim Using Phased Array Ultrasonic Examination. Master's thesis. Chungnam National University, Daejeon, Korea.
- KSNT, 2013. Phased Array Ultrasonic Technology Application, Yongsan, Seoul, Korea.
- Lee, J.K., 2014. Technology Applications of Advanced Phased Array Ultrasonic, Heavy and Chemical Facilities Safety Inspection Center. Chonnam National University, Gwangju, Korea.
- NAVSEA, 1997. Requirements for Fabrication, Welding, and Inspection of Submarine Structure. Report No. T9074-AD-GIB-010/16881997. Commander Naval Sea Systems Command, Washington D.C., USA.
- Olympus NDT, 2004. Technology Applications of Advanced Phased Array Ultrasonic. Waltham, USA.
- Sehwa, 2001. Unabridged Dictionary on Chemistry. Paju, Korea.
- Yule, Peter, Woolner, Derek, 2008. The collins class submarine story – steel, spies and spin. North. Mar. 18 (2), 150–151.